Geoscience Frontiers 6 (2015) 605–615

HOSTED BY

Contents lists available at ScienceDirect

China University of Geosciences (Beijing)

Geoscience Frontiers

journal homepage: www.elsevier.com/locate/gsf

Research paper

Changing provenance of late Cenozoic sediments in the Jianghan Basin

Lei Shao [a,b], Shengyuan Yuan [b,c], Chang'an Li [b,d,*], Chunguo Kang [e], Wenjing Zhu [f], Yindi Liu [b], Jietao Wang [a,b]

[a] Wuhan Center of Geological Survey, China Geological Survey, Wuhan 430205, China
[b] Faculty of Earth Sciences, China University of Geosciences, Wuhan 430074, China
[c] College of Urban Planning & Environment Science, Xuchang University, Xuchang 461000, China
[d] State Key Laboratory of Biogeology and Environmental Geology, Wuhan 430074, China
[e] Institute of Geophysics & Geomatics, China University of Geosciences, Wuhan 430074, China
[f] Hubei Institute of Geological Sciences, Wuhan 430034, China

ARTICLE INFO

Article history:
Received 13 November 2013
Received in revised form
2 April 2014
Accepted 17 April 2014
Available online 23 May 2014

Keywords:
Yangtze River
Jianghan Basin
Trace element
REE
Provenance

ABSTRACT

The Yangtze River is one of the most important components of the East Asia river system. In this study, sediments in the Jianghan Basin, middle Yangtze River, were selected for trace element and rare earth element (REE) measurements, in order to decipher information on the change of sediment provenance and evolution of the Yangtze River. According to the elemental variations, the late Cenozoic sediments of the Jianghan Basin could be divided into four parts. During 2.68–2.28 Ma and 1.25–0 Ma, provenance of the sediments was consistent, whereas sediments were derived from variable sources during 2.28–1.25 Ma. Comparison of the elemental compositions between the Pliocene and Quaternary sediments revealed a change in sediment source from a more felsic source area to a more basic source area around the Pliocene–Quaternary boundary. Input from the Emeishan LIP should account for this provenance change. Based on the provenance analysis of sediments in the Jianghan Basin, we infer that the Yangtze River developed into a large river with its drainage basin extended to the Emeishan LIP no later than the Pliocene–Quaternary boundary.

1. Introduction

Research of large rivers has been highlighted in recent years, especially the rivers draining the southeastern Tibetan Plateau (Brookfield, 1998; Clark et al., 2004; Clift et al., 2006, 2008a, b; Yang et al., 2006, 2007a; Liang et al., 2008; Kong et al., 2009; Shao et al., 2012). These large rivers transport large amount of terrestrial materials to the marginal seas and thus are considered as important linkage between the continents and oceans (Clift et al., 2004; Zheng and Jia, 2009). Evolution of these large rivers can be correlated to the uplift of the mountains and plateaus where these large rivers originate. The process of orogeny is proposed to profoundly affect the global climate system (An et al., 2001). So reconstructing the "Source to Sink" process of sediments from these rivers plays an important role in understanding the global change and its regional response.

The Yangtze River (Fig. 1) is typical not only because of its large drainage area but also the complicated geological background. Its drainage basin consists of complex strata from Archean to Quaternary. The Emeishan Large Igneous Province is the typical basic source in the upper Yangtze especially in the Jinshajiang valley. Quaternary loose sediments and Paleozoic sedimentary rocks widely outcrop in the middle–lower reaches of the Yangtze River (Fig. 2). The Emeishan Large Igneous Province widely distributes at the west margin of the Yangtze Craton. It occupies an area over 250,000 km^2 and is one of the most important igneous provinces in the world (Xiao et al., 2004). As pointed by Yang et al. (2007a), it is suffered strongly chemical weathering under the influence of humid and warm climate and thus should have much influence on the

* Corresponding author. Faculty of Earth Sciences, China University of Geosciences, Wuhan 430074, China.
E-mail addresses: chanli_cug@sohu.com, chanli@cug.edu.cn (C. Li).
Peer-review under responsibility of China University of Geosciences (Beijing)

http://dx.doi.org/10.1016/j.gsf.2014.04.010

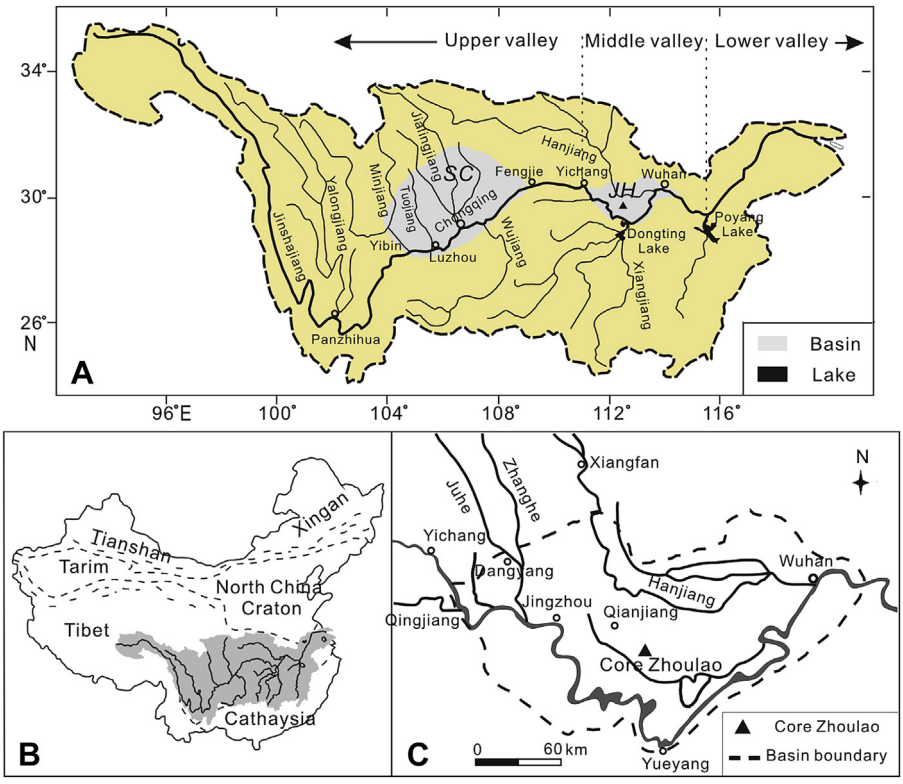

Figure 1. The Yangtze drainage basin and location of the Jianghan Basin and the Core Zhoulao (modified after Yang et al., 2007a; Zhang et al., 2008). A: The Yangtze drainage basin with the location of the Sichuan Basin and Jianghan Basin. SC and JH denote the Sichuan Basin and Jianghan Basin respectively. B: A sketch of Chinese tectonic units. C: Simplified geological map of the Jianghan Basin and the location of the Core Zhoulao.

geochemical composition of the river sediments. Thus, the Emeishan LIP is important for discussing the provenance of the core sediments in the Jianghan Basin and the evolution of the Yangtze River. Study of the evolution of the Yangtze River has a long history of more than 100 years (Willis and Blackwelder, 1907; Li, 1933; Li and Zhang, 1997; Brookfield, 1998; Li et al., 2001; Yang and Li, 2001; Clark et al., 2004; Fan et al., 2005; Clift et al., 2006, 2008b; Yang et al., 2006; Xiang et al., 2007; Huang et al., 2009; Kang et al., 2009; Kong et al., 2009; van Hoang et al., 2009; Jia et al., 2010; Richardson et al., 2010; Shao et al., 2012). Clark et al. (2004) proposed that the Yangtze River was once the tributary of the so called “paleo-Red River” draining into the South China Sea and reorganized by sequential river capture and reversal events. The Nd evolution in the Hanoi Basin showed that the middle Yangtze (downstream of the first bend) was once important source to the paleo-Red River and was lost from the paleo-Red River

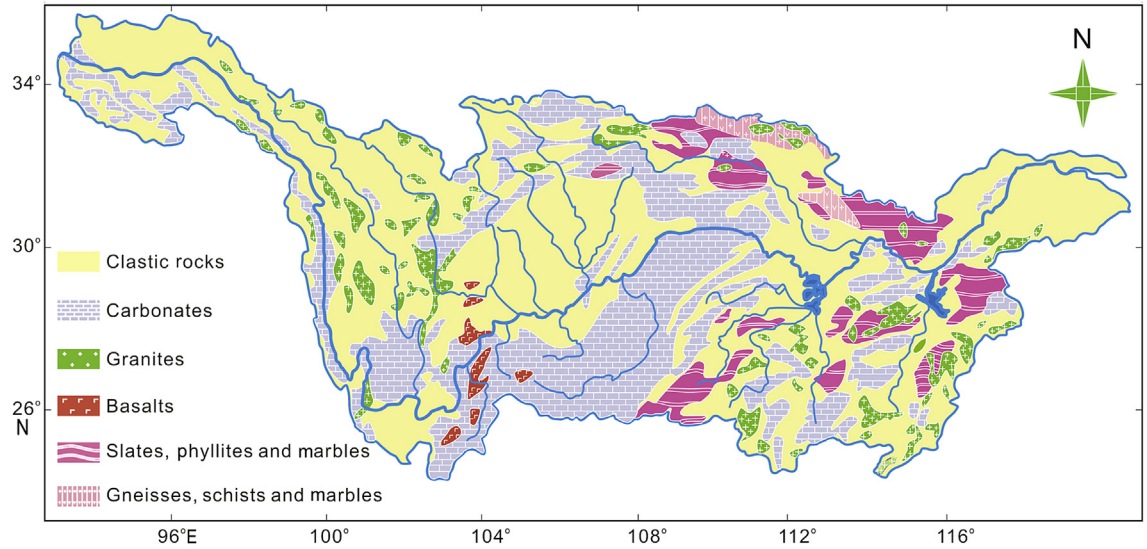

Figure 2. Regional geological map of the Yangtze River drainage basin (modified after Kang et al., 2009). It showed the complicated compositions of lithology in the Yangtze drainage and the location of the largely distributed Emeishan basalts.

between 37 and 24 Ma (Clift et al., 2006). Nd, Pb data and U-Pb dating and Hf isotope analysis of zircons support the paleo-drainage pattern that the Songpan-Garze terrain once belonged to the paleo-Red drainage basin and was gone before 12 Ma or maybe much earlier (Clift et al., 2006, 2008b; van Hoang et al., 2009). However no compelling evidence for the connection between the upper Yangtze (upstream of the first bend) and the paleo-Red River were found, but their data do not preclude this possibility (van Hoang et al., 2009). Recently many important researches based on the theory of "Source to Sink" have been carried out in the Yangtze Delta and the Jianghan Basin to reconstruct the evolutionary history of the Yangtze River. These authors used the elemental compositions (Yang et al., 2006, 2007b; Huang et al., 2009), isotopic compositions (Yang et al., 2007b), and age patterns of monazite (Fan et al., 2005; Yang et al., 2006) and zircon (Jia et al., 2010) to trace the source of the late Cenozoic sediments in the Yangtze Delta. Their research provided direct evidence of evolution of the Yangtze River and showed that the wide Yangtze drainage basin similar as today's dimension was formed mainly at the beginning of the Quaternary. As revealed by rare earth element (REE) and Neodymium isotopic compositions, the ancient Yangtze River might have undergone different evolution phases under the tectonic-climatic coupling controls (Yang et al., 2007b). Heavy mineral compositions of sediments in the Jianghan Basin revealed that the sediments after 1.1 Ma show stable heavy mineral compositions were similar as the modern Yangtze River (Kang et al., 2009). Besides, magnetism parameters characters of these sediments were also similar to the modern Yangtze River (Zhang et al., 2008). These researches argue that the provenance of the sediments in the Jianghan Basin has been the same as the modern upper Yangtze River since 1.1 Ma. This change of provenance was also identified in the Neodymium isotopic variations (Shao et al., 2012). However, the Neodymium isotopic variations also recorded the changing provenance around the beginning of the Quaternary and unstable provenance of the early and middle Pleistocene sediments. Therefore, more evidence is needed to decipher the provenance implications recorded in the late Cenozoic sediments in the Jianghan Basin.

The immobile elements, such as Y, Zr, Hf, Th, Sc, Co, Cr, REEs and their ratios have been found to be least affected by geological processes including weathering, transport and sorting. Thus, these elements and their ratios can be useful indicators of provenance (Taylor and McLennan, 1985; Fralick and Kronberg, 1997). Immobile elements La and Th are relatively enriched in felsic igneous rocks whereas Co and Sc are concentrated in mafic rocks. Thus, ratios such as La/Sc and Co/Th could be used to make distinction between felsic and basic sources. Just as mentioned above, the Emeishan LIP is most typical basic source in the upper Yangtze drainage basin, thus the elemental compositions could be used to identify the provenance changes of the core sediments in the Jianghan Basin, especially whether these sediments were influenced by the Emeishan LIP. In this paper, sediments taken from the Core Zhoulao in the Jianghan Basin were selected for elemental analysis. The main purpose of our paper is to examine variations in elemental compositions and identify the changing provenance of the late Cenozoic sediments in the Jianghan Basin. Additionally, we try to provide more constraints on the evolution of the Yangtze River.

2. River setting and study area

2.1. River setting and geological background of the Yangtze drainage basin

The Yangtze River flows from west to east to debouch into the East China Sea. It is located between 24°27′–35°44′ N and 90°33′–122°19′ E (Fig. 1), with the drainage basin area of 1.94×10^6 km^2 (Chen et al., 2001). The huge Yangtze drainage basin can be divided into three parts, the upper, middle and lower reaches.

The upper Yangtze is from the source to Yichang, with an area of 100×10^4 km^2. This section of the Yangtze River is joined by some large tributaries: the Yalongjiang, Minjiang, Tuojiang, Jialingjiang and Wujiang. Hydrological records reveal that most of the sediment load in the Yangtze drainage basin is derived from the upper basin (Chen et al., 2001).

The middle Yangtze is from Yichang to Hukou, jointed by the Dongting Lake drainage basin, Hanjiang and Poyang Lake drainage basin. The Hanjiang is the longest tributary and join the Yangtze River at Wuhan.

The lower Yangtze is segment of the river below Hukou. Several large interior lakes, such as the Chaohu Lake and Taihu Lake in association with many tributaries, drain into the lower Yangtze River. Quaternary loose sediments and Paleozoic sedimentary rocks widely outcrop in the middle–lower reaches.

The Yangtze drainage basin consists of complex strata from Archean to Quaternary (Fig. 2). Quaternary loose sediments widely outcrop in the Jianghan Basin and its surrounding area. Triassic flysh and Neoproterozoic–Permian passive margin sediments widely outcrop at the Longmenshan area. Paleozoic carbonate rocks, Mesozoic red clastic rocks and igneous rocks largely distributed in the drainage basins of the Jinshajiang and Wujiang rivers. In spite of the complex source rocks, the Emeishan Large Igneous Province (Emeishan LIP), covers a large area of over 250,000 km^2 (Xiao et al., 2004) is the typical basic source in the upper Yangtze especially in the Jinshajiang valley. It suffered strongly chemical weathering under the influence of humid and warm climate and thus should have much influence on the geochemical compositions of the river sediments. Therefore, it should be a major supplier of basic sources to the Jianghan Basin.

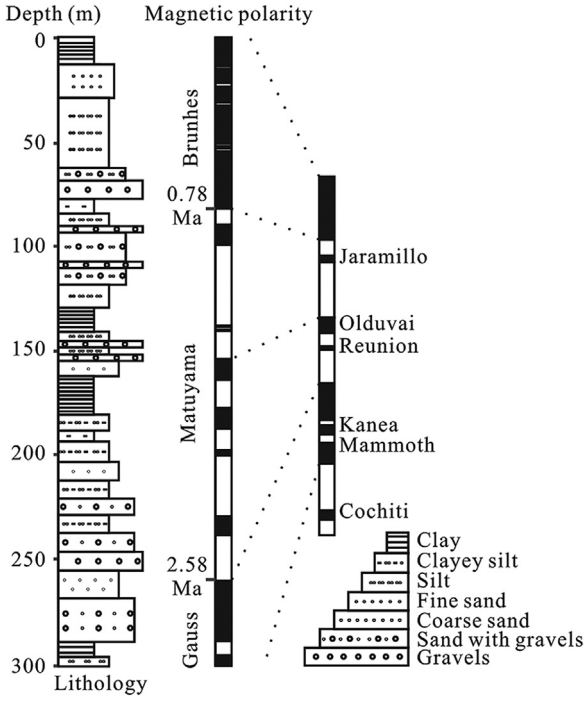

Figure 3. Magnetic polarity and lithology of the late Cenozoic sediments in the Jianghan basin. Data were collected from Zhang et al. (2008).

Table 1
Trace element (in ppm) compositions of sediments in the Jianghan Basin.

Depth (m)	Li	Be	Sc	V	Cr	Co	Ni	Cu	Zn	Ga	Rb
8.50	41.59	2.34	13.96	112.15	91.12	16.20	42.88	46.80	82.12	18.13	115.46
26.00	36.17	2.26	12.62	112.10	85.40	27.02	46.84	35.84	85.30	16.32	103.90
38.10	37.96	2.08	13.34	107.13	89.28	16.66	41.92	31.34	80.34	16.60	104.68
46.00	36.23	2.13	12.49	108.96	82.88	35.22	50.43	37.31	97.24	15.28	86.71
53.00	34.69	1.96	12.93	115.05	75.50	24.72	45.84	34.46	84.99	16.61	94.14
56.30	39.69	2.33	14.01	117.07	87.77	29.22	57.07	36.11	96.55	17.68	100.30
62.00	45.83	2.39	14.55	133.79	92.01	26.85	59.56	38.06	107.13	18.34	119.90
72.00	37.04	1.99	12.23	93.99	75.74	13.53	35.67	54.07	70.26	14.79	90.88
82.00	40.13	2.03	12.58	97.16	82.10	16.52	43.03	45.55	72.17	15.83	96.90
87.20	38.87	2.06	13.87	123.22	116.01	23.77	50.15	32.86	79.56	17.28	96.04
94.60	42.25	2.05	13.10	103.18	83.76	14.64	39.92	42.41	78.14	16.77	104.83
97.40	31.54	1.92	12.40	109.99	92.26	21.88	45.73	33.27	80.15	16.35	82.78
105.40	39.42	2.40	16.37	133.00	106.99	21.07	49.59	35.62	81.00	17.98	99.22
107.80	38.77	1.85	12.69	104.21	91.80	15.45	44.05	44.24	74.70	14.94	89.04
117.60	33.04	1.81	12.84	118.65	90.21	27.36	57.17	37.17	76.54	15.21	85.10
121.00	34.48	1.80	11.77	87.60	80.59	13.06	38.06	39.55	65.14	13.72	88.69
122.10	43.24	2.05	12.52	98.68	78.30	15.25	42.04	61.40	80.74	15.82	103.35
129.80	25.68	1.84	10.02	82.30	63.44	14.03	30.37	40.75	65.58	12.17	87.47
132.10	34.35	1.84	11.99	91.91	76.21	14.25	37.59	38.54	76.96	14.84	94.87
137.80	38.05	2.79	14.10	118.18	81.45	25.25	56.54	32.75	89.87	16.99	95.21
143.00	32.22	1.76	13.19	122.90	109.19	21.20	48.51	32.54	78.91	15.72	85.04
148.30	32.85	1.86	12.15	134.18	91.68	30.03	58.14	33.33	82.39	16.05	83.67
151.00	32.50	1.70	13.24	127.46	98.68	23.77	54.66	40.73	76.27	16.11	83.61
155.00	34.14	2.04	17.88	167.75	111.56	23.62	56.93	37.99	82.33	16.77	83.47
160.90	18.98	1.40	8.10	61.02	49.94	9.86	23.97	51.03	40.89	8.61	50.49
163.60	38.39	1.78	12.36	96.59	75.83	13.70	35.35	43.25	71.43	14.12	87.99
167.20	35.05	2.45	15.17	125.93	98.86	21.11	47.30	26.83	82.28	18.78	89.22
170.00	39.69	1.76	12.56	98.13	77.28	15.20	39.71	44.07	76.34	14.99	93.89
173.70	30.18	1.67	14.00	126.25	118.38	22.65	54.11	27.77	81.37	15.76	75.63
179.20	35.22	1.92	10.79	76.86	60.94	12.22	28.21	36.77	60.69	12.52	93.25
183.80	43.09	1.79	11.04	88.92	70.47	11.45	29.17	73.77	76.11	15.67	110.71
193.70	20.35	1.22	11.39	91.02	137.24	11.96	31.02	26.91	56.11	12.91	65.05
198.60	41.10	1.87	12.20	92.02	85.80	13.00	37.85	39.90	69.60	14.60	96.50
205.00	34.70	1.88	13.60	120.00	111.00	20.70	55.65	30.70	80.20	15.40	82.20
208.20	27.60	1.60	14.15	121.00	115.00	22.05	55.60	24.02	73.70	13.80	65.30
214.80	17.60	1.43	10.80	103.00	72.58	22.90	46.30	20.70	61.90	11.60	54.80
233.50	29.00	1.76	12.40	119.00	90.10	21.05	49.50	33.30	81.10	15.20	83.10
243.30	33.60	1.83	13.40	117.00	97.30	19.00	49.30	29.10	78.30	16.20	86.60
254.70	34.30	1.90	14.60	134.00	102.00	21.60	50.30	23.90	78.60	17.20	84.10
266.10	32.30	2.32	13.10	115.00	99.70	19.30	45.40	40.90	87.40	16.60	87.70
271.40	32.50	2.18	11.30	91.60	101.00	12.70	36.10	26.50	67.50	14.10	78.80
279.40	33.80	1.98	11.70	105.00	88.00	16.90	43.10	24.80	72.50	15.70	89.90
286.00	40.00	3.75	13.90	121.00	88.40	45.00	106.00	81.70	101.00	18.80	107.00
287.00	37.90	2.46	11.60	97.50	79.60	16.20	51.80	61.90	91.90	15.80	101.00
296.00	26.50	1.42	11.30	97.80	122.00	13.30	43.60	27.20	63.20	14.40	74.60
300.00	26.10	1.55	11.20	88.70	126.00	12.30	36.70	23.51	57.60	12.70	66.90

Depth (m)	Sr	Y	Zr	Nb	Cs	Ba	Hf	Ta	Pb	Th	U
8.50	183.95	28.35	198.51	16.18	7.62	529.28	5.26	1.18	19.62	12.22	2.53
26.00	221.45	27.15	183.37	14.75	5.83	549.18	5.02	1.13	27.05	11.09	2.40
38.10	212.59	30.71	280.46	17.34	6.15	494.60	7.50	2.28	21.23	14.29	2.95
46.00	205.02	29.35	258.51	14.98	6.38	508.69	6.92	1.10	29.37	13.77	2.79
53.00	247.28	25.84	186.79	15.56	4.80	543.07	4.97	1.15	21.43	11.38	2.43
56.30	215.58	30.04	265.49	17.79	6.11	564.00	7.16	1.32	26.54	12.45	2.84
62.00	168.41	29.25	248.93	17.77	7.59	521.99	6.49	1.30	24.03	12.20	2.70
72.00	190.39	30.00	200.24	15.42	5.98	371.40	5.22	1.11	19.30	11.89	2.68
82.00	177.44	28.82	208.72	15.35	6.62	390.73	5.47	1.11	19.22	12.02	2.71
87.20	217.47	30.75	292.91	17.65	5.25	488.27	7.63	1.25	26.51	12.61	2.80
94.60	173.96	30.93	225.35	16.10	6.81	401.58	5.93	1.16	20.21	13.72	2.89
97.40	223.61	30.90	199.15	16.08	3.88	436.01	5.14	1.16	20.17	11.29	2.22
105.40	198.06	32.74	353.76	16.68	5.47	446.61	9.29	1.23	27.15	14.76	3.27
107.80	191.83	29.97	238.34	16.41	6.12	342.92	6.30	1.16	19.51	12.20	2.94
117.60	215.38	28.32	220.94	15.28	3.92	496.15	5.82	1.10	37.75	10.29	2.29
121.00	161.15	30.48	290.36	15.62	5.63	328.88	7.97	1.23	20.06	14.46	3.20
122.10	163.35	32.57	222.93	16.18	7.13	371.04	5.95	1.27	22.53	14.10	3.15
129.80	159.55	23.65	251.12	12.48	4.27	500.36	6.62	0.78	18.94	18.84	3.02
132.10	185.36	30.24	238.00	16.61	6.01	461.27	6.30	1.25	19.01	13.21	2.94
137.80	173.25	27.45	265.36	15.05	5.42	466.33	6.95	1.12	27.17	10.58	2.64
143.00	209.87	30.55	502.80	17.01	4.58	528.66	13.28	1.26	31.07	12.96	3.05
148.30	224.07	27.83	277.34	16.75	4.19	498.66	7.25	1.21	23.95	11.26	2.21
151.00	225.07	27.31	274.98	16.39	3.84	497.26	7.23	1.15	29.31	10.68	2.14
155.00	188.16	32.02	418.39	16.59	4.56	399.90	10.63	1.19	25.84	13.44	2.71
160.90	119.77	21.39	181.04	9.31	3.45	199.43	4.57	0.68	13.36	7.08	1.90
163.60	186.67	31.77	274.37	16.07	5.62	346.27	6.99	1.10	17.49	12.49	2.61
167.20	255.62	28.26	335.59	16.71	4.82	615.87	8.92	1.22	29.29	11.68	2.48

Table 1 (*continued*)

Depth (m)	Sr	Y	Zr	Nb	Cs	Ba	Hf	Ta	Pb	Th	U
170.00	167.99	30.75	237.04	16.18	6.08	349.76	6.19	1.16	19.55	13.77	2.71
173.70	252.86	28.32	398.97	16.25	3.74	668.12	10.23	1.23	25.84	10.39	2.46
179.20	48.79	30.30	404.76	17.19	7.02	315.36	10.62	1.36	21.26	15.46	3.26
183.80	55.99	31.94	479.71	17.61	8.28	349.80	12.82	1.43	28.37	17.95	3.54
193.70	133.05	36.45	924.38	17.09	3.51	282.40	24.05	1.26	17.32	17.08	3.49
198.60	149.07	32.49	371.91	17.12	6.69	333.10	9.74	1.34	17.73	15.23	3.40
205.00	277.12	27.21	339.05	16.28	4.32	712.06	8.71	1.18	22.47	11.34	2.48
208.20	460.10	26.94	347.00	15.49	3.39	1280.45	9.18	1.09	24.04	11.28	2.17
214.80	796.62	22.06	160.74	12.28	2.74	2216.94	4.37	0.89	24.62	6.73	1.43
233.50	337.05	26.25	197.69	15.13	4.29	871.43	5.26	1.11	24.73	8.80	1.93
243.30	193.86	29.31	392.36	16.28	4.15	396.19	10.26	1.18	23.54	13.04	2.55
254.70	206.63	29.03	314.37	16.16	4.12	407.33	8.28	1.17	24.28	11.81	2.39
266.10	233.20	28.31	366.36	17.57	4.26	447.69	9.86	1.26	24.66	12.96	2.83
271.40	132.34	32.01	483.49	17.06	4.80	378.97	12.78	1.23	18.30	12.53	3.22
279.40	179.37	29.58	279.23	15.45	4.41	411.07	7.27	1.11	23.19	10.22	2.41
286.00	83.32	33.30	216.45	15.82	8.15	303.67	5.78	1.19	44.91	13.80	3.76
287.00	62.40	29.97	31.00	0.04	6.91	281.98	0.93	0.00	22.10	10.27	1.82
296.00	136.94	33.87	805.07	21.06	4.00	311.75	21.17	1.55	18.83	16.49	3.63
300.00	183.34	43.09	746.99	19.80	3.49	290.51	19.13	1.42	17.84	18.15	3.73

2.2. Geological background of the Jianghan Basin and the late Cenozoic sediments in Core Zhoulao

The Jianghan Basin is located between 29°26′–30°23′ N and 111°30′–114°32′ E, in the middle Yangtze River (Fig. 1). It is a Cretaceous–early Tertiary rift basin, situated between the Qinling belt on the north and the Sichuan–Yangtze belt on the south. The Yangtze River runs through the Jianghan Basin from west to east. Quaternary loose sediments widely outcrop inside the basin and its surrounding area. Tectonic frameworks of the Jianghan Basin are controlled by two groups of tensional normal faults lying NNW and EW, respectively. The basin has subsided ever since the late Cretaceous (Zhang, 1994). The Jianghan Basin is surrounded by hills, the Dahong Mountain and Dabie Mountain on the north, the Mufu Mountain on the east and Exi Mountain (Exi means the west Hubei Province) on the west. Such a geological controlled basin is favorable to siltation (Yin et al., 2007). The thickness of the Neogene deposits varies between 300 and 600 m while that of the Quaternary deposits varies within a range of 250–300 m (Li and Zhang, 1997). With continuous deposits ever since the late Cenozoic, the Jianghan Basin provides ideal materials for the research of the evolution of the Yangtze River.

The continuously drilled core (Core Zhoulao) was taken in the Qianjiang Depression, at the depocenter of the Jianghan Basin. The final drilling depth was 300.49 m, with the average recovery of 85%. Zhang et al. (2008) reported the magnetic stratigraphic framework of Core Zhoulao. The Brunhes/Matuyama boundary (~0.78 Ma) and Matuyama/Gauss (~2.58 Ma) boundary were located at the depths of 82 m and 260 m respectively. The Jaramillo (0.99–1.07 Ma) and Olduvai (1.77–1.95 Ma) normal polarity subepoch were located at the depths of 90–100 m and 154.99–164.37 m respectively, while the Reunion normal polarity subepoch (2.14–2.15 Ma) was located at the depth of 178.69–185.07 m. The Quaternary strata of the Jianghan Basin primarily consist of fluvial facies interbedded with lacustrine facies and comprise several major fining-upward and coarsening-upward sediment sequences (Zhang et al., 2008, Fig. 3).

3. Materials and analytical methods

3.1. Sampling

A total of 46 samples were collected from the borehole sediments. Fine-grained clastic sediments can best reflect the average composition of the large source area, so only the fine fraction (<0.058 mm) was selected for the determination of trace and rare earth element (REE) concentrations. The <0.058 mm fine fraction was washed to remove salts and sieved from the bulk sediments using a 250-mesh sieve in deionized water and dried at room temperature in a clean oven. Then the dried samples were grounded into powder <200 mesh with an agate mortar. Most of the samples were previously analyzed for Nd isotopic compositions (Shao et al., 2012).

3.2. Laboratory procedures

An aliquot of 50 ± 1 mg of powdered sample was moistened with a few drops of ultrapure water in a teflon bomb and added with 1.5 mL HNO_3 + 1.5 mL HF. The sealed bomb was heated at 190 ± 5 °C in oven for >48 h. After the solution was evaporated at 140 °C to dryness, 1 mL HNO_3 was added and the solution was evaporated to dryness again. The resultant salt was re-dissolved by adding 3 mL 30% HNO_3 and heated in the bomb at 190 ± 5 °C in oven for >12 h. The final solution was transferred into a polyethylene bottle and diluted to ~100 g with mixture of 2% HNO_3 for ICP-MS analysis. Concentrations of trace and rare earth elements (REE) were measured using an inductive coupled plasma mass spectrometer (ICP-MS: Agilent 7500a) at the State Key Laboratory of Geological Processes and Mineral Resources (GPMR), China University of Geosciences. Analytical precision and accuracy were monitored by standards AGV-2, BHVO-2, BCR-2 and RGM-1. The results indicate that the relative deviations between measured and certified values are generally less than 5% for most elements and ~10% for some transitional elements.

4. Results

4.1. Trace element

Table 1 presents trace elements concentrations of the sediments from the Core Zhoulao. Generally, the trace elements show large variations downward in Core Zhoulao (Fig. 4), with an average coefficient of variation of 23%. Some elements such as Sr, Zr, Ba and Hf yield coefficient of variation higher than 50%. The element Zr shows the highest coefficient of variation, concentration of which varies between 31 and 924.4 ppm. While the element Y shows stable concentration with a coefficient of variation of 12% (Fig. 5a).

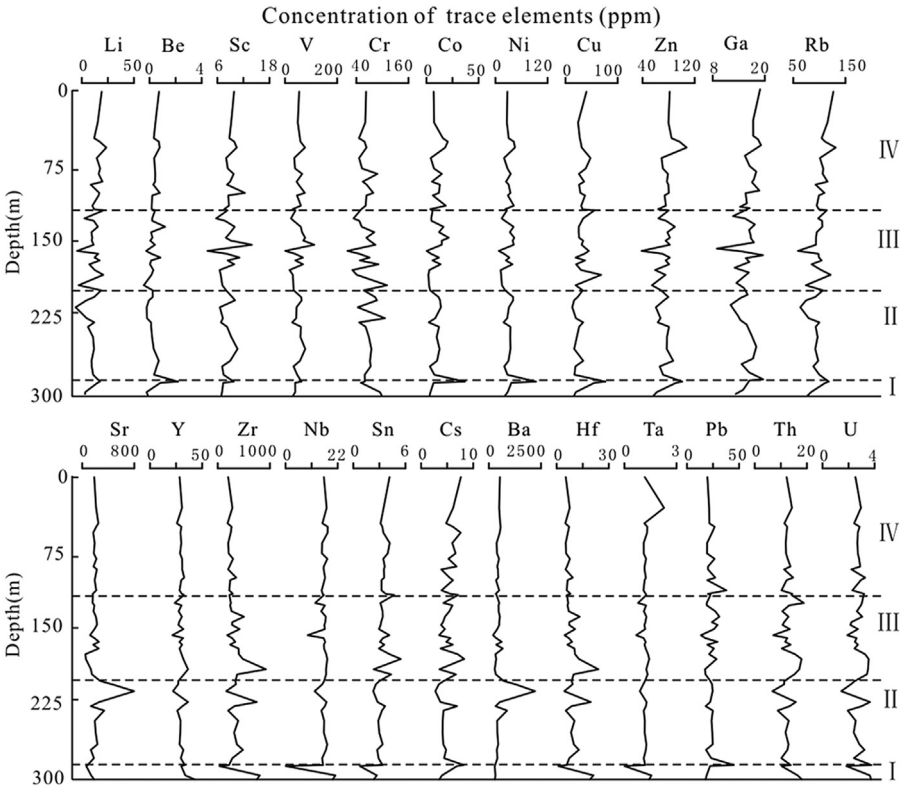

Figure 4. Depth variations of trace element concentrations in the <0.058 mm fraction of Core Zhoulao.

The upper continental crust (UCC) (Taylor and McLennan, 1985) normalized pattern for trace elements (average concentration of each element is taken to represent the trace elemental composition of the sediments in Core Zhoulao) indicates that the sediments are depleted in Be, Ga, Sr and Ba. In contrast to the above set of elements, the sediments show enrichment of Li, Y, Hf, Ta, Nb, Zr, Cu, Zn, Cr, Co, and Ni compared to UCC (Fig. 5b).

In order to make it easier to show the variations of the trace element compositions, we divided the sediments into four parts (Age of the sediments were presumed based on magnetic stratigraphic framework of Core Zhoulao):

Part I (300–287 m, 2.77–2.68 Ma): Trace elemental compositions are much different from the other parts. Some elements are characterized by extremely high or low concentrations, such as Be, Co, Ni, Cu, Pb and Nb.
Part II (287–205 m, 2.68–2.28 Ma) and Part IV (117–0 m, 1.25–0 Ma): Trace element compositions of sediments from these two parts show similar and the least fluctuant variations.
Part III (205–117 m, 2.28–1.25 Ma): Most of the trace elements from this part show the most fluctuant variations except Nb and Ta.

4.2. Rare earth element (REE)

The REE concentrations of sediments from Core Zhoulao are listed in Table 2 and Fig. 6. In Fig. 7 we show the chondrite (Anders and Grevess, 1989) normalized REE pattern of the sediments from the core. As might be expected, the chondrite normalized REE patterns are characterized by steep light-REE (LREE) and relatively flat heavy-REE (HREE), which are similar to those of UCC (Taylor and McLennan, 1985).

In general, the total REE of the sediments ranges between 117.7 and 321.2 ppm with an average of 197.8 ppm. The ratios of LREE/HREE in sediments vary from 5.79 to 11.73, suggesting that LREEs are enriched when compared with HREEs. $(La/Yb)_N$ varies between 5.71 and 11.87, with an average of 8.23. $(La/Sm)_N$ varies between 2.72 and 4.52, with an average of 3.55, indicating medium LREE fractionation.

Negative anomalies of Ce (δCe) and Eu (δEu) with large variations are present in the core sediments. The δCe ratios range between 0.76 and 0.97, with an average of 0.83, indicating a slight

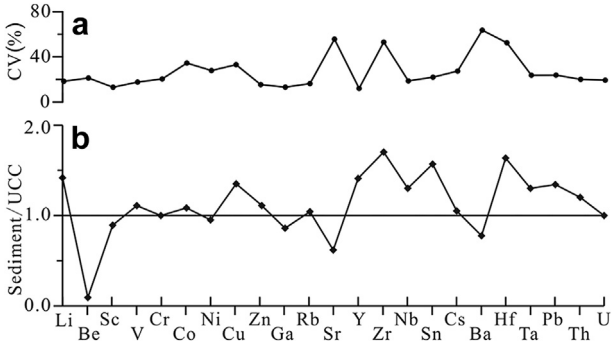

Figure 5. Coefficient of variation (a) and UCC normalized trace element pattern (b) of sediments from Core Zhoulao. CV denotes coefficient of variation. Data of UCC are collected from Taylor and McLennan (1985). The average concentration of each element is taken to represent the trace elemental composition of the sediments in Core Zhoulao.

Table 2
REE compositions of sediments in the Jianghan Basin. Eu anomaly (δEu) is calculated by $Eu_N/(Sm_N \times Gd_N)^{1/2}$ and Ce anomaly (δCe) by $Ce_N/(La_N \times Pr_N)^{1/2}$, with normalization to chondrite. Chondrite values used are from Anders and Grevess (1989).

Depth (m)	La	Ce	Pr	Nd	Sm	Eu	Gd	Tb	Dy	Ho	Er
8.50	33.93	69.40	8.05	30.38	6.05	1.32	5.66	0.83	4.84	1.03	2.79
26.00	34.02	80.54	8.31	32.18	6.23	1.35	5.60	0.90	5.02	0.98	2.88
38.10	39.46	77.96	9.23	34.25	6.98	1.37	6.11	0.91	5.34	1.10	3.08
46.00	38.74	87.51	9.27	36.70	7.27	1.38	6.51	0.98	5.45	1.01	2.96
53.00	34.64	71.85	8.27	31.03	6.37	1.42	5.64	0.81	4.66	0.94	2.56
56.30	36.12	72.80	8.50	32.04	6.45	1.40	5.93	0.89	5.23	1.10	3.02
62.00	36.50	74.13	8.65	33.23	6.88	1.46	6.05	0.88	4.98	1.07	2.84
72.00	36.02	71.55	8.25	30.87	6.39	1.34	5.73	0.84	5.05	1.06	2.84
82.00	34.77	70.29	8.14	30.21	6.28	1.31	5.69	0.84	4.87	1.04	2.81
87.20	38.31	75.41	8.84	33.49	6.76	1.48	5.95	0.88	5.18	1.12	3.07
94.60	37.29	74.15	8.59	32.25	6.55	1.40	6.00	0.88	5.17	1.09	2.93
97.40	35.66	71.27	8.36	31.64	6.63	1.44	5.97	0.86	5.16	1.09	2.89
105.40	45.62	91.07	10.79	40.45	8.06	1.62	6.83	0.99	5.75	1.18	3.20
107.80	36.56	73.55	8.71	32.17	6.76	1.38	5.80	0.85	5.02	1.05	2.81
117.60	33.61	68.39	7.95	30.26	6.14	1.36	5.58	0.80	4.80	1.00	2.66
121.00	39.06	77.80	9.05	33.42	6.70	1.37	6.06	0.89	5.38	1.10	2.98
122.10	38.84	77.95	9.03	33.21	6.66	1.34	6.15	0.91	5.50	1.14	3.09
129.80	33.93	68.09	7.97	29.19	6.10	1.25	5.11	0.73	4.10	0.86	2.26
132.10	36.49	73.33	8.62	32.26	6.55	1.39	5.94	0.86	5.28	1.07	2.90
137.80	31.54	61.72	7.49	27.52	5.95	1.34	5.39	0.77	4.76	0.98	2.59
143.00	38.44	76.81	9.15	33.98	7.00	1.48	6.33	0.92	5.50	1.12	3.10
148.30	34.86	71.13	8.54	31.64	6.67	1.41	5.93	0.85	5.11	1.02	2.75
151.00	37.47	74.60	8.92	32.96	7.02	1.51	5.90	0.84	5.00	0.99	2.69
155.00	43.77	86.49	10.47	39.17	8.18	1.70	7.07	1.00	5.94	1.18	3.27
160.90	25.18	47.19	5.71	21.41	4.32	0.87	4.03	0.57	3.44	0.70	1.94
163.60	38.32	76.52	8.98	33.15	6.85	1.40	6.03	0.89	5.38	1.07	3.02
167.20	37.41	73.21	8.64	32.08	6.69	1.48	5.79	0.84	5.07	1.00	2.77
170.00	40.92	80.67	9.53	35.24	7.26	1.45	6.42	0.91	5.47	1.12	3.02
173.70	34.88	69.73	8.19	31.11	6.50	1.56	5.91	0.87	5.04	1.02	2.79
179.20	38.06	76.39	8.81	31.92	6.42	1.16	5.81	0.87	5.36	1.15	3.23
183.80	41.76	83.16	9.63	34.69	6.93	1.23	5.92	0.89	5.46	1.17	3.31
193.70	54.70	111.14	12.89	47.11	9.09	1.62	7.71	1.09	6.44	1.34	3.70
198.60	38.98	77.36	9.30	34.79	7.00	1.45	6.46	0.95	5.64	1.20	3.25
205.00	38.31	76.16	9.19	34.41	6.68	1.55	6.00	0.84	4.86	0.99	2.70
208.20	37.59	75.45	9.17	34.24	7.05	1.60	6.20	0.86	4.90	1.00	2.72
214.80	24.84	51.41	6.28	24.34	4.95	1.44	4.76	0.69	4.00	0.82	2.20
233.50	31.05	62.45	7.46	28.46	5.82	1.41	5.38	0.81	4.81	0.97	2.66
243.30	43.13	85.49	10.08	37.28	7.11	1.59	6.45	0.92	5.22	1.03	2.85
254.70	40.72	83.43	9.85	37.23	7.48	1.58	6.33	0.90	5.40	1.05	2.78
266.10	41.03	80.76	9.71	35.99	7.23	1.56	6.08	0.86	5.04	1.05	2.79
271.40	40.62	82.35	9.49	35.29	6.71	1.36	6.00	0.88	5.37	1.14	3.17
279.40	34.41	67.83	8.12	30.18	6.02	1.37	5.34	0.83	5.19	1.06	2.85
286.00	51.13	235.55	13.94	53.30	11.75	2.42	9.42	1.37	7.83	1.44	3.73
287.00	38.03	74.12	8.98	33.77	6.86	1.39	6.11	0.87	5.07	0.98	2.52
296.00	57.78	116.22	13.70	50.40	9.47	1.79	7.45	1.07	6.06	1.25	3.52
300.00	57.00	114.63	13.56	49.91	9.89	1.76	8.23	1.21	7.19	1.49	4.20

Depth (m)	Tm	Yb	Lu	δCe	δEu	$(La/Yb)_N$	$(Gd/Yb)_N$	ΣREE
8.50	0.42	2.71	0.41	1.03	0.69	8.99	1.73	167.83
26.00	0.43	2.62	0.42	1.15	0.69	9.59	1.77	182.48
38.10	0.46	2.87	0.44	1.00	0.64	9.87	1.76	189.57
46.00	0.47	2.75	0.45	1.11	0.61	10.41	1.96	201.45
53.00	0.37	2.34	0.37	1.04	0.72	10.62	2.00	171.27
56.30	0.45	2.89	0.45	1.02	0.69	8.97	1.70	177.28
62.00	0.43	2.78	0.42	1.02	0.69	9.42	1.80	180.29
72.00	0.41	2.77	0.42	1.02	0.68	9.32	1.71	173.55
82.00	0.42	2.63	0.39	1.02	0.67	9.50	1.79	169.68
87.20	0.46	2.92	0.44	1.00	0.71	9.40	1.69	184.32
94.60	0.44	2.86	0.43	1.02	0.68	9.36	1.73	180.02
97.40	0.42	2.60	0.39	1.01	0.70	9.85	1.90	174.37
105.40	0.48	3.06	0.45	0.99	0.66	11.01	1.85	219.49
107.80	0.45	2.85	0.41	1.01	0.68	9.19	1.68	178.39
117.60	0.42	2.69	0.39	1.03	0.71	8.97	1.72	166.04
121.00	0.46	2.98	0.42	1.01	0.66	9.40	1.68	187.67
122.10	0.48	3.00	0.44	1.02	0.64	9.27	1.69	187.76
129.80	0.35	2.23	0.33	1.02	0.68	10.90	1.89	162.52
132.10	0.45	2.76	0.43	1.01	0.68	9.48	1.78	178.32
137.80	0.41	2.62	0.40	0.98	0.72	8.65	1.70	153.47
143.00	0.48	3.18	0.47	1.00	0.68	8.68	1.65	187.96
148.30	0.42	2.54	0.39	1.01	0.69	9.85	1.93	173.25
151.00	0.40	2.49	0.38	1.00	0.72	10.78	1.96	181.15
155.00	0.47	3.05	0.45	0.99	0.68	10.30	1.92	212.23
160.90	0.29	1.78	0.26	0.96	0.64	10.16	1.88	117.68

(*continued on next page*)

Table 2 (*continued*)

Depth (m)	Tm	Yb	Lu	δCe	δEu	$(La/Yb)_N$	$(Gd/Yb)_N$	ΣREE
163.60	0.45	2.75	0.42	1.01	0.67	10.00	1.82	185.23
167.20	0.40	2.73	0.39	1.00	0.73	9.84	1.76	178.50
170.00	0.44	2.80	0.42	1.00	0.65	10.48	1.90	195.67
173.70	0.41	2.63	0.40	1.01	0.77	9.51	1.86	171.03
179.20	0.50	3.37	0.48	1.02	0.58	8.11	1.43	183.53
183.80	0.54	3.47	0.54	1.02	0.59	8.64	1.41	198.70
193.70	0.58	3.96	0.59	1.03	0.59	9.90	1.61	261.97
198.60	0.47	3.18	0.47	1.00	0.66	8.79	1.68	190.49
205.00	0.38	2.61	0.39	1.00	0.75	10.52	1.90	185.07
208.20	0.39	2.55	0.38	1.00	0.74	10.58	2.01	184.08
214.80	0.31	1.96	0.28	1.01	0.90	9.09	2.01	128.29
233.50	0.38	2.42	0.35	0.99	0.65	10.22	1.76	235.34
243.30	0.43	2.85	0.42	1.01	0.64	10.10	1.67	196.03
254.70	0.42	2.76	0.40	1.01	0.77	9.22	1.84	154.42
266.10	0.41	2.78	0.41	1.01	0.72	10.87	1.88	204.85
271.40	0.52	3.26	0.50	1.02	0.70	10.59	1.90	200.32
279.40	0.43	2.84	0.41	0.99	0.72	10.60	1.81	195.70
286.00	0.60	3.85	0.54	1.03	0.65	8.94	1.52	196.64
287.00	0.36	2.15	0.30	1.00	0.74	8.68	1.55	166.88
296.00	0.56	3.71	0.57	1.01	0.65	11.17	1.66	273.54
300.00	0.66	4.33	0.67	1.01	0.60	9.44	1.57	274.73

depletion. Whereas, Eu shows a distinct depletion, with δEu ratios ranging between 0.58 and 0.98.

Part I (300–287 m, 2.77–2.68 Ma): REE compositions are much different from the other parts. Some samples are characterized by extremely high REE concentration.
Part II (287–205 m, 2.68–2.28 Ma) and Part IV (117–0 m, 1.25–0 Ma): REE compositions of sediments from these two parts show similar variations, which are the least fluctuant.
Part III (205–117 m, 2.28–1.25 Ma): Sediments of this part show fluctuant REE concentrations.

5. Discussion

5.1. Provenance discrimination based upon trace element and REE compositions

The immobile elements, such as Th, Sc, Co, REEs and their ratios have been found to be at least affected by geological processes including weathering, transport and sorting. Thus, these elements and their ratios can be useful indicators of provenance (Taylor and McLennan, 1985; Fralick and Kronberg, 1997). Immobile elements La and Th are relatively enriched in felsic igneous rocks whereas Co and Sc are concentrated in mafic rocks. Thus, ratios such as La/Sc

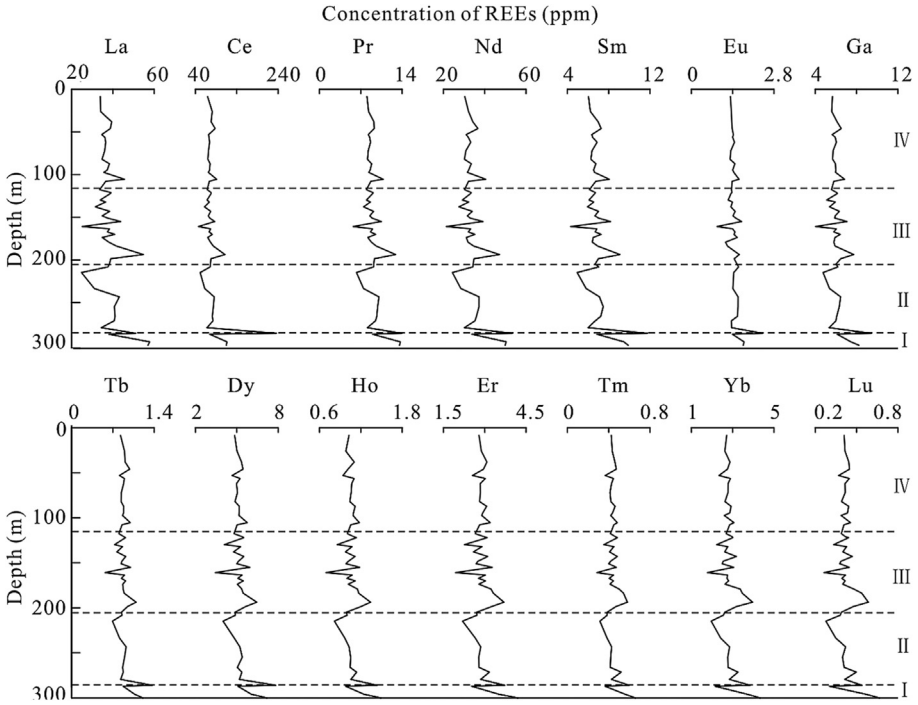

Figure 6. Depth variations of REE concentrations in the <0.058 mm fraction of Core Zhoulao. Noticed that variations of the REEs are similar to those of the trace elements.

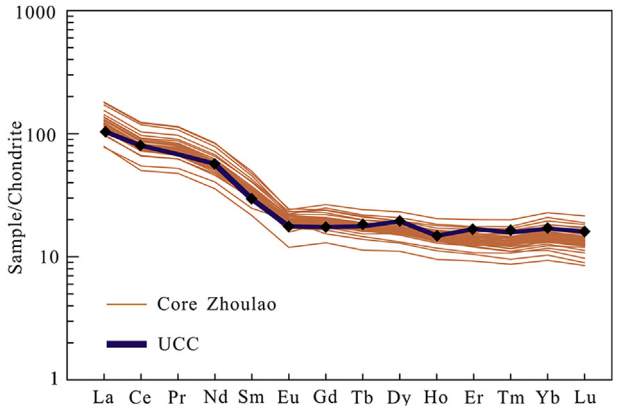

Figure 7. Chondrite normalized REE patterns of the sediments in the <0.058 mm fraction of Core Zhoulao and the UCC. UCC and Chondrite values are from Taylor and McLennan (1985) and Anders and Grevess (1989) respectively.

and Co/Th could be used to make distinction between felsic and basic sources.

Observation of the sediment lithology shows that the significant trace element and REE compositions cannot be well correlated with particular sediment lithology or its variation. Significant geochemical variations still exist even among sediments with same characters. Therefore changing sediment characters were not expected to affect the geochemical variations.

As shown by Fig. 8, the sediments below the depth of 287 m are characterized by lower Co/Th and higher La/Sc ratios. It is evident that lower Co/Th and higher La/Sc ratios in sediments indicate more felsic source rock compositions in the provenances. Therefore we infer that the sediments of the Core Zhoulao below the depth of 287 m primarily originated from more felsic sources whereas sediments of the upper part were derived from more mafic sources.

Comparison between the Pliocene and Quaternary sediments revealed the changing sediment sources from felsic provenances to more basic provenances around 2.68 Ma. Similar provenance change could also be found in the Yangtze Delta (Fig. 9). The Yangtze drainage basin consists of complex strata from Archean to Quaternary. Quaternary loose sediments widely outcrop in the Jianghan Basin and its surrounding area. Triassic flysh and Neoproterozoic–Permian passive margin sediments widely outcrop at

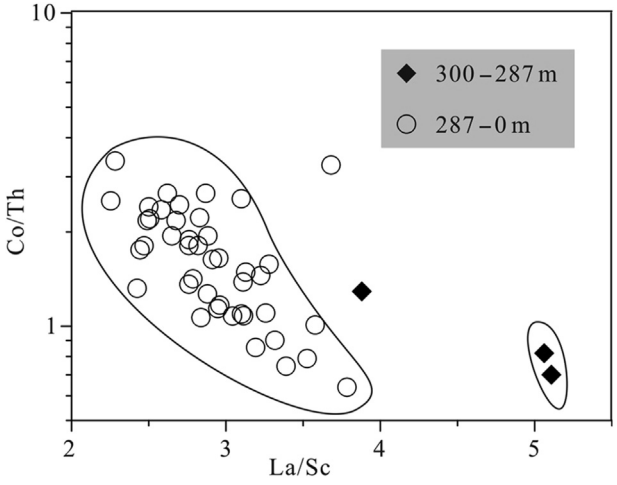

Figure 8. Plots of Co/Th vs. La/Sc for sediments from Core Zhoulao. Sediments below 287 m could be separated from the other part, with lower Co/Th and higher La/Sc ratios.

the Longmenshan area. Paleozoic carbonate rocks, Mesozoic red clastic rocks and igneous rocks largely distributed in the drainage basins of the Jinshajiang and Wujiang rivers. In spite of the complex source rocks, the Emeishan Large Igneous Province (Emeishan LIP), which covers a large area over 250,000 km^2 (Xiao et al., 2004) is the typical basic source in the upper Yangtze especially in the Jinshajiang valley. It suffered strongly chemical weathering under the influence of humid and warm climate and thus should have much influence on the geochemical compositions of the river sediments. Therefore, it should be a major source of mafic sediment to the Jianghan Basin. The elemental compositions could not provide compelling evidence for the detailed provenance of sediments below the depth of 287 m. However, only the contribution of the Emeishan LIP could induce the changing provenance from more felsic to more mafic. So what can be confirmed is that the source area of the sediments in the Jianghan Basin had extended to the Emeishan LIP no later than the Pliocene–Quaternary boundary.

5.2. Constraint on the evolution of the Yangtze River

Previous studies proposed that the Yangtze River could be dated back to the Cretaceous or the Tertiary (Li, 1933; Clift et al., 2006, 2008b; Huang et al., 2009; van Hoang et al., 2009; Jia et al., 2010; Richardson et al., 2010), the early Quaternary (Li and Zhang, 1997; Li et al., 2001; Yang and Li, 2001; Yang et al., 2006, 2007b; Zhang et al., 2008; Kang et al., 2009; Kong et al., 2009; Shao et al., 2012) or the late Pleistocene (Brookfield, 1998; Chen et al., 2009).

As our borehole does not go deep enough, so it cannot provide more details on the river evolution history before. Just as the discussion above, the trace element and REE compositions suggest the provenance of sediments in the Jianghan Basin extended to the Emeishan LIP no later than the Pliocene–Quaternary boundary. Based on this we infer that the Yangtze River developed into a large river similar as the modern Yangtze no later than the beginning of the Quaternary. What needed to be declared is that we do not try to prove a young birth to the Yangtze River, we just conclude that the birth of the Yangtze River should predate the Pliocene–Quaternary boundary.

Besides the Jianghan Basin, sediments in the Yangtze Delta also recorded information on the evolution of the Yangtze River. Yang et al. (2006) reported the elemental compositions and monazite age patterns of sediments in the Yangtze Delta and proposed that the Yangtze River developed into a large river similar to today's scale during the early Quaternary at >1.18 Ma. Huang et al. (2009) also found that provenance of the sediments in the Yangtze Delta had changed greatly from felsic sources to mafic sources since the late Pliocene (approximately at 3.1 Ma). Research of the stepped landforms in the Three Gorges area revealed that the ancestral Yangtze River began to adjust its drainage network and ran through the Three Gorges during 3.6 and 1.8 Ma (Li et al., 2001). These researches are consistent with our research.

5.3. Changing patterns of erosion in the Yangtze valley

Sediments of Part II (287–205 m) and Part IV (117–0 m) show stable and similar trace element and REE compositions (Figs. 2 and 4), indicating stable and similar sources of these sediments. It indicates that the patterns of erosion were stable during those times.

Whereas, sediments of Part III (205–117 m) show fluctuant trace element and REE compositions (Figs. 2 and 4) indicating fluctuant sources. Heavy mineral compositions of sediments in the Jianghan Basin revealed that the sediments of Part IV (117–0 m) showed stable heavy mineral compositions and were similar as the modern Yangtze (Kang et al., 2009). Besides, magnetism parameters characters of these sediments were also similar to the modern Yangtze

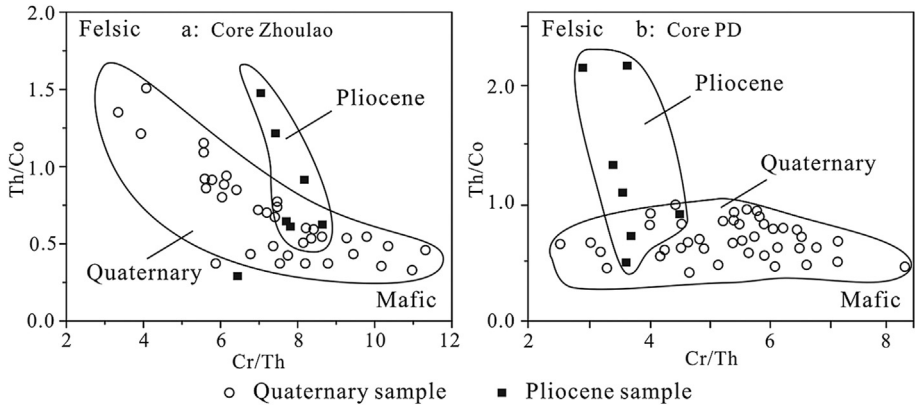

Figure 9. Comparison of the provenance change between the Jianghan Basin and the Yangtze Delta. It revealed that information on the provenance change around the Pliocene–Quaternary boundary was recorded in sediments of both the Jianghan Basin and the Yangtze delta. Data of the Yangtze Delta are collected from Yang et al. (2007b).

River (Zhang et al., 2008). However, these researches provided little information on the fluctuant sources of sediments of Part III (205–117 m, 2.28–1.25 Ma) as revealed by the elemental compositions (this paper). Therefore geochemical compositions could provide more constraints on the source of the Quaternary sediments in the Jianghan Basin. As discussed above, the source area of the sediments in the Jianghan Basin had extended to the upper valley including the Emeishan LIP no later than the Pliocene–Quaternary boundary. Then the unstable provenance of the sediments could only be explained as the result of the unstable patterns of erosion in the drainage basin especially in the upper Yangtze.

Sun (2005) reported loess provenance also had a pronounced provenance shift across the Pliocene–Quaternary boundary, which was attributed to increased erosion of Asian mountains caused by colder climate. The possibility that more materials were input to the Jianghan Basin from the Emeishan due to onset of the intensive Northern Hemisphere glaciations cannot be excluded based on the present data. However, the only way that the materials from the Emeishan LIP could be delivered and deposited in the Jianghan Basin was through the Yangtze River. It did show that the Emeishan LIP had been part of the Yangtze drainage basin ever since the Pliocene–Quaternary boundary.

Issues such as recycling, non-unique sources, and pre- and post-depositional modifications may complicate interpretation of results from individual provenance techniques. The best way to circumvent these issues in provenance studies is to use integrated methods (Nie et al., 2012; Van Eynatten and Dunkl, 2012). In our previous studies we have reported the Neodymium isotopic compositions of the late Cenozoic sediments in the Jianghan Basin (Shao et al., 2012). The Nd isotopes show similar variations as the elemental compositions reported in this study. It also recorded the information on the provenance expansion around the Pliocene–Quaternary boundary and the unstable patterns of erosion in the upper Yangtze drainage basin during the early Pleistocene.

6. Conclusions

Trace element and REE compositions of the sediments from Core Zhoulao in the Jianghan Basin were presented to identify the provenance change and to provide useful constraints on the evolution of the Yangtze River. According to the elemental variations, the late Cenozoic sediments of the Jianghan Basin could be divided into four parts. Comparison between the Pliocene and Quaternary sediments revealed the changing sediment sources from more felsic provenances to more basic provenances around the Pliocene–Quaternary boundary. Input from the Emeishan LIP should account for this provenance change. Based on this provenance change, we infer that the Yangtze River developed into a large river with its drainage basin extended to the Emeishan LIP no later than the Pliocene–Quaternary boundary.

Acknowledgments

This work was supported by the National Natural Science Foundation of China (Grants Nos. 40971008 and 40771213) and the Open Research Program of State Key Laboratory of Loess and Quaternary Geology (Grant No. SKLLQG0908).

References

An, Z.S., Kutzbach, J.E., Prell, W.L., Porter, S.C., 2001. Evolution of Asian monsoons and phased uplift of the Himalaya–Tibetan plateau since late Miocene times. Nature 411, 62–66.

Anders, E., Grevess, N., 1989. Abundances of the elements – Meteoritic and solar. Geochimica et Cosmochimica Acta 53, 197–214.

Brookfield, M.E., 1998. The evolution of the great river systems of southern Asia during the Cenozoic India-Asia collision: rivers draining southwards. Geomorphology 22, 285–312.

Chen, J., Wang, Z., Chen, Z., Wei, Z., Wei, T., Wei, W., 2009. Diagnostic heavy minerals in Plio-Pleistocene sediments of the Yangtze coast, China with special reference to the Yangtze River connection into the sea. Geomorphology 113, 129–136.

Chen, Z.Y., Li, J.F., Shen, H.T., Wang, Z.H., 2001. Yangtze River of China: historical analysis of discharge variability and sediment flux. Geomorphology 41, 77–91.

Clark, M.K., Schoenbohm, L.M., Royden, L.H., Whipple, K.X., Burchfiel, B.C., Zhang, X., Tang, W., Wang, E., Chen, L., 2004. Surface uplift, tectonics, and erosion of eastern Tibet from large-scale drainage patterns. Tectonics 23, TC1006. http://dx.doi.org/10.1029/2002TC001402.

Clift, P.D., Blusztajn, J., Duc, N.A., 2006. Large-scale drainage capture and surface uplift in eastern Tibet-SW China before 24 Ma inferred from sediments of the Hanoi Basin, Vietnam. Geophysical Research Letters 33, L19403. http://dx.doi.org/10.1029/2006GL027772.

Clift, P.D., Campbell, I.H., Pringle, M.S., Carter, A., Zhang, X.F., Hodges, K.V., Khan, A.A., Allen, C.M., 2004. Thermochronology of the modern Indus River bedload: new insight into the controls on the marine stratigraphic record. Tectonics 23, TC5013. http://dx.doi.org/10.1029/2003TC001559.

Clift, P.D., Ellam, R.M., Hinton, R., Tan, M.T., 2008a. Pb, Sr and Nd isotopic constraints on the evolving provenance of the Red River. Geochimica et Cosmochimica Acta 72 (Suppl. 1), A168–A168.

Clift, P.D., Van Long, H., Hinton, R., Ellam, R.M., Hannigan, R., Tan, M.T., Blusztajn, J., Duc, N.A., 2008b. Evolving east Asian river systems reconstructed by trace element and Pb and Nd isotope variations in modern and ancient Red River-Song Hong sediments. Geochemistry, Geophysics, Geosystems 9, Q04039. http://dx.doi.org/10.1029/2007GC001867.

Fan, D.D., Li, C.X., Kazumi, Y., Zhou, B.C., Li, B.H., Wang, Q., Yang, S.Y., Deng, B., Wu, G.X., 2005. Monazite age spectra in the late Cenozoic strata of the Changjiang delta and its implication on the Changjiang run-through time. Science in China Series D: Earth Sciences 48, 1718–1727.

Fralick, P.W., Kronberg, B.I., 1997. Geochemical discrimination of elastic sedimentary rock sources. Sedimentary Geology 113, 111–124.

Huang, X.T., Zheng, H.B., Yang, S.Y., Xie, X.J., 2009. Investigation of sedimentary geochemistry of core DY03 in the Yangtze Delta: implications to tracing provenance. Quaternary Sciences 29, 299–307 (in Chinese with English abstract).
Jia, J.T., Zheng, H.B., Huang, X.T., Wu, F.Y., Yang, S.Y., Wang, K., He, M.Y., 2010. Detrital zircon U-Pb ages of late Cenozoic sediments from the Yangtze delta: implication for the evolution of the Yangtze River. Chinese Science Bulletin 55, 1520–1528.
Kang, C.G., Li, C.A., Wang, J.T., Shao, L., 2009. Heavy minerals characteristics of sediments in Jianghan Plain and its indication to the forming of the Three Gorges. Earth Science-Journal of China University of Geosciences 34, 419–427 (in Chinese with English abstract).
Kong, P., Granger, D.E., Wu, F.Y., Caffee, M.W., Wang, Y.J., Zhao, X.T., Zheng, Y., 2009. Cosmogenic nuclide burial ages and provenance of the Xigeda paleo-lake: implications for evolution of the middle Yangtze River. Earth and Planetary Science Letters 278, 131–141.
Li, C.A., Zhang, Y.F., 1997. Geoscientific factors analyses on the through cutting of main drainages and the formation of flood damage in China. Exploration of Nature 16, 61–65 (in Chinese with English abstract).
Li, C.Y., 1933. Development of the upper Yangtze. Geological Society of China Bulletin 13, 107–117.
Li, J.J., Xie, S.Y., Kuang, M.S., 2001. Geomorphic evolution of the Yangtze Gorges and the time of their formation. Geomorphology 41, 125–135.
Liang, Y.H., Chung, S.L., Liu, D.Y., Xu, Y.G., Wu, F.Y., Yang, J.H., Wang, Y., Lo, C.H., 2008. Detrital zircon evidence from Burma for reorganization of the eastern Himalayan river system. American Journal of Science 308, 618–638.
Nie, J., Horton, B.K., Saylor, J.E., Mora, A., Mange, M., Garzione, C.N., Basu, A., Moreno, C.J., Caballero, V., Parra, M., 2012. Integrated provenance analysis of a convergent retroarc foreland system: U-Pb ages, heavy minerals, Nd isotopes, and sandstone compositions of the Middle Magdalena Valley basin, northern Andes, Colombia. Earth-Science Reviews 110, 111–126.
Richardson, N.J., Densmore, A.L., Seward, D., Wipf, M., Yong, L., 2010. Did incision of the Three Gorges begin in the Eocene? Geology 38, 551–554.
Shao, L., Li, C.A., Yuan, S.Y., Kang, C.G., Wang, J.T., Li, T., 2012. Neodymium isotopic variations of the late Cenozoic sediments in the Jianghan Basin: implications for sediment source and evolution of the Yangtze River. Journal of Asian Earth Sciences 45, 57–64.
Sun, J., 2005. Nd and Sr isotopic variations in Chinese eolian deposits during the past 8 Ma: implications for provenance change. Earth and Planetary Science Letters 240, 454–466.
Taylor, S.R., McLennan, S.M., 1985. The Continental Crust: its Composition and Evolution. Blackwell, Oxford.
Van Eynatten, H., Dunkl, I., 2012. Assessing the sediment factory: the role of single grain analysis. Earth-Science Reviews 115, 97–120.
van Hoang, L., Wu, F.Y., Clift, P.D., Wysocka, A., Swierczewska, A., 2009. Evaluating the evolution of the Red River system based on in situ U-Pb dating and Hf isotope analysis of zircons. Geochemistry Geophysics Geosystems 10, Q1108. http://dx.doi.org/10.1029/2009GC002819.
Willis, B., Blackwelder, E., 1907. Research in China, vol. 1. Press of Gibson Brothers, Washington, pp. 278–339.
Xiang, F., Zhu, L.D., Wang, C.S., Zhao, X.X., Chen, H.D., Yang, W.G., 2007. Quaternary sediment in the Yichang area: implications for the formation of the Three Gorges of the Yangtze River. Geomorphology 85, 249–258.
Xiao, L., Xu, Y.G., Mei, H.J., Zheng, Y.F., He, B., Pirajno, F., 2004. Distinct mantle sources of low-Ti and high-Ti basalts from the western Emeishan large igneous province, SW China: implications for plume-lithosphere interaction. Earth and Planetary Science Letters 228, 525–546.
Yang, D.Y., Li, X.S., 2001. Study on the eastward flow of the Jinsha River. Journal of Nanjing University Natural Sciences 37, 317–322 (in Chinese).
Yang, S.Y., Jiang, S.Y., Ling, H.F., Xia, X.P., Sun, M., Wang, D.J., 2007a. Sr-Nd isotopic compositions of the Changjiang sediments: implications for tracing sediment sources. Science in China Series D-Earth Sciences 50, 1556–1565.
Yang, S.Y., Li, C.X., Yokoyama, K., 2006. Elemental compositions and monazite age patterns of core sediments in the Changjiang Delta: implications for sediment provenance and development history of the Changjiang River. Earth and Planetary Science Letters 245, 762–776.
Yang, S.Y., Wei, G.J., Xia, X.P., Sun, M., Tang, M., 2007b. Provenance study of the late Cenozoic sediments in the Changjiang delta: REE and Nd isotopic constraints. Quaternary Sciences 27, 339–346 (in Chinese).
Yin, H., Liu, G., Pi, J., Chen, G., Li, C., 2007. On the river-lake relationship of the middle Yangtze reaches. Geomorphology 85, 197–207.
Zhang, D.H., 1994. Neotectonics and Quaternary environmental changes in Jianghan Basin. Crustal Deformation and Earthquake 14, 74–80 (in Chinese).
Zhang, Y.F., Li, C.A., Wang, Q.L., Chen, L., Ma, Y.F., Kang, C.G., 2008. Magnetism parameters characteristics of drilling deposits in Jianghan Plain and indication for forming of the Yangtze River Three Gorges. Chinese Science Bulletin 53, 584–590.
Zheng, H.B., Jia, J.T., 2009. Geological evolution of big river systems and tectonic control. Quaternary Sciences 29, 268–275 (in Chinese with English abstract).